

Multifunctional Smart Window based on Dielectric Elastomer Actuator

Milan Shrestha ^{1,*}, Gih-Keong Lau ², Anand Asundi ³ and Zhenbo Lu ⁴

¹ Temasek Laboratories, National University of Singapore, Singapore 117411;

² Department of Mechanical Engineering, National Chiao Tung University, Taiwan 30010;

³ School of Mechanical and Aerospace Engineering, National University of Singapore, Singapore 639798;

⁴ School of Aeronautics and Astronautics, Sun Yat-Sen University, P. R. China, 510275;

* Correspondence: milan001@e.ntu.edu.sg; Tel.: +65-83600602

Abstract: Soft actuators are the compliant material-based devices capable of producing large deformation upon external stimuli. Dielectric elastomer actuators (DEA) are a type of soft actuators that operate on voltage stimuli. Apart from soft robotics, these actuators can serve many novel applications, for example, tunable optical gratings, lens, diffusers, smart windows and so on. This article presents our current work on tunable smart windows which can regulate the light transmittance and the sound absorption. This smart window can promote daylighting while maintaining privacy by electrically switching between transparent and opaque. As a tunable optical surface scatters, it turns transparent with smooth surfaces like a flat glass; but it turns 'opaque' (translucent) with the micro-rough surface. The surface roughness is varied employing surface micro-wrinkling or unfolding using dielectric elastomer actuation. In addition, this smart window is equipped with another layer of transparent micro-perforated dielectric elastomer actuator (DEA), which acts like Helmholtz resonators serving as a tunable and broader sound absorber. It can electrically tune its absorption spectrum to match the noise frequency for maximum acoustic absorption. The membrane tension and perforation size are tuned using DEA activation to tune its acoustic resonant frequency. Such a novel smart window can be made as cheap as glass due to its simple all-solid-state construction. In future, they might be used in smart green building and could potentially enhance the urban livability.

Keywords: Dielectric elastomer actuators; smart windows; smart acoustic absorbers; transparent thin films, micro-wrinkling.

1. Introduction

Glass panels are widely used as transparent facades to buildings. They are optically transparent to allow daylighting while being acoustic barriers, they isolate the outdoor noise. However, these transparent glasses make the privacy of the buildings vulnerable. In addition, the glass panels are not effective to damp out the indoor noise or echo that reverberate in the events of indoor musical performance or public announcement. Therefore, there is a need for window solutions that can regulate visibility and sufficiently absorb sound as well. Curtains are the simplest solution to achieve both functionalities. Thick textile curtains are often used to block visibility for privacy purpose. They can also act like porous acoustic absorbers to attenuate the indoor noise.[1] Yet, they are unable to provide both functionalities sufficiently and simultaneously. For example, they cannot absorb sound when they are open to allow daylighting. There are few translucent sound-absorbing curtains, [2] but they are relatively poor at sound absorption and they still block visibility.

There are different types of glasses which provide either one of these functionalities. For example, there are smart window solutions that can switch between transparent and opaque or translucent as desired. These commercial smart windows are based on electrochromic [3,4], polymer-dispersed liquid crystal (PDLC) devices [5,6] and suspended particle devices (SPD) [7].

Electrochromic devices in a battery construction change colour and thus light absorption coefficient upon electrical stimuli. PDLC devices consist of the liquid crystals immersed in the polymer matrix. The random orientations of these liquid crystals are electrically controlled to switch between milky and clear states. SPD has light-absorbing particles whose distribution is also electrically controlled to adjust the transmission of light. But, these devices are costly to adopt for large-area windows [3]. Their manufacturing cost is high (\$200 per square foot) due to complex construction. Besides, their adoption is hindered by other issues. For example, electrochromic windows are subjected a slow response (taking 5 minutes for switching a 0.01 square meter panel) and fast ageing; whereas, PLDC and SPD only shows a moderate transparency tuning range (50%-80%) and are not so transparent at its clear state [7]. Moreover, they continuously consume high power when switched to be transparent. Low cost transparency switching devices based on tunable optical diffuser seems promising, but reported devices are far from applicable due to large strain involvement and narrow tuning range. [8-12]

Similarly, there are few transparent glass solutions to minimize reverberation of indoor noise. [13-15] For example, panel absorbers can be transparent, but they have a narrow absorption frequency bandwidth. [16] Microperforated panel (MPP) absorbers have slightly broader absorption frequency bandwidth. But they are still fixed and are unable to absorb sound beyond their absorption bandwidth. These passive absorbers are inefficient when absorbing sound that outlies their absorption bandwidth and are unable to adapt to varying noise frequency.

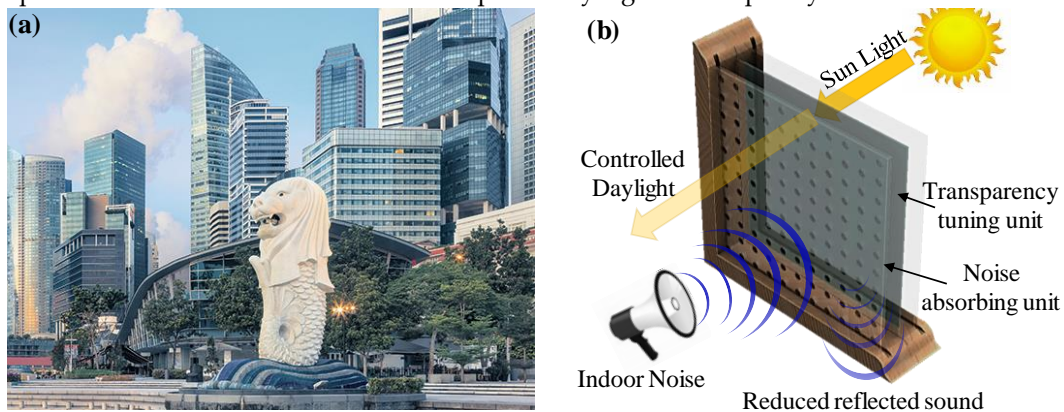


Figure 1. (a) Use of many glass facades in most building in modern cities; (b) Schematic of the smart window made of two components, first component can tune its transparency and second can absorb broader band noise while adapting to the varying noise frequency.

Currently, no window appliance can regulate natural daylight in a building, tune the transparency for privacy and sufficiently absorb indoor noise to reduce its reverberation simultaneously at a reasonable price. The article presents a concept of such low-cost smart window based on dielectric elastomer actuators (DEAs). This work explores micro-wrinkling of hybrid multilayer electrode made of metal oxide thin film and polymeric conductive thin films. It is used to develop a tunable optical diffuser which requires a low activation strain for transparency switching. This elastomeric tunable optical diffuser shall meet the stringent requirements for high transmittance in the clear state, a very low transmittance at the translucent state, fast response, and long life for repeated cycles. In addition, this work addresses the need for the transparent and tunable broadband acoustic absorber. We used transparent micro-perforated membranes to make a relatively broadband acoustic absorber. Also, the dielectric elastomer actuator is used to make this absorber tunable. Hence, they can tune their absorption spectrum and maintain optimal absorption of the noise with changing dominant frequency. Eventually, these two DEAs based components are combined for two functionalities. The first layer provides the transparency switching capability and the second layer provides the tunable broadband noise absorption (see **Figure 1(b)**).

2. Theory

This article presents DEA for two functionalities. First, it shows transparency tuning device made of tunable optical diffuser consisting of two tunable optical scatterer surfaces sandwiching a dielectric elastomer membrane (see **Figure 2(a-b)**). Its surface topography change can tune the scattering of forward visible light.[17,18] For a smooth surface, the total transmittance at normal incidence is: $T = 1 - R = \frac{4n_1n_2}{(n_2+n_1)^2}$ according to Fresnel equations. Consider a device with two identical Gaussian surfaces of voltage-tunable roughness $\sigma(V)$ and finite electrical conductivity. The specular (non-diffuse) part of the total transmittance through the device is obtained as:[19-21]

$$T_{spec} = T^2 \cdot \exp \left\{ -2 \left[\frac{2\pi\sigma(V)}{\lambda} (n_1 - n_2) \right]^2 \right\} \quad (1)$$

where $n_1=1$ for air and n_2 being greater than 1 for elastomer substrate. The surface roughens upon formation of microwrinkle under biaxial compression. Dielectric elastomer actuation can unfold this initially microwrinkled surfaces of compliant electrodes. Application of high voltage V across the dielectric membrane of thickness t_s induces a compressive electrostatic pressure $P_e = \epsilon_r \epsilon_0 (V/t_s)^2$, where ϵ_r is the dielectric constant and ϵ_0 is the permittivity of vacuum [22,23]. Due to Poisson's ratio effect, electrostatically squeezed membrane expands in the area. Hence, this voltage-induced areal expansion can reduce the compressive strain in the thin-film electrodes. Consequently, it reduces the surface roughness turning the membrane optically clear.

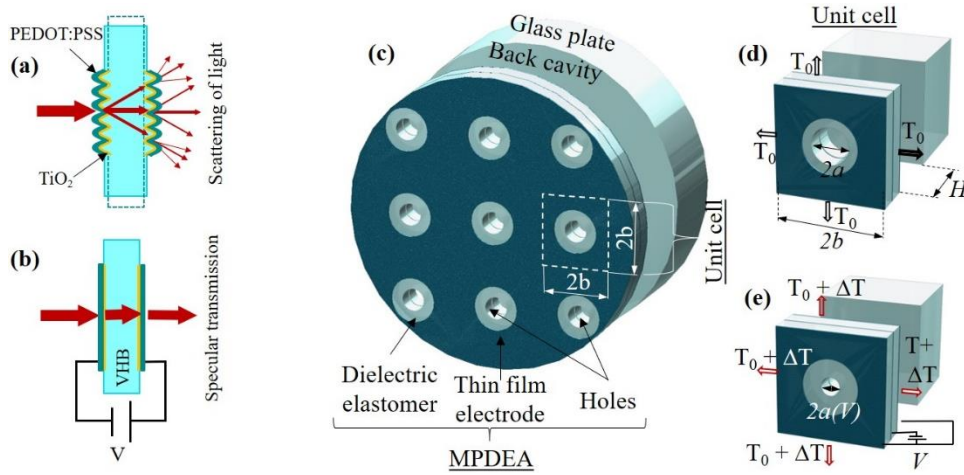


Figure 2. Schematic of the transparency tuning device based on DEA optical scatterer (a) optically scattering state at inactive state; (b) Optically transparent state at activated state. (c) Schematic of the MPDEA device; (d) magnified view of a hole of the MPDEA at the inactive state; (e) a hole of the MPDEA at activated state.

Second, this article presents a smart transparent acoustic absorber consisting of a micro-perforated dielectric elastomer actuator (MPDEA) and a 40mm deep back-cavity. The MPDEA consists of a micro-perforated membrane of dielectric elastomer sandwiched by a pair of transparent polymeric compliant electrodes. The high voltage activation of MPDEA reduces the bi-axial pre-stress T_0 in the membrane by $\Delta T(V)$ such that the remaining tension becomes

$$T = T_0 - \Delta T(V) = T_0 - \frac{\nu}{1 - \nu} P_e, \quad (2)$$

where ν is the Poisson's ratio of dielectric elastomer membrane according to Ref.[24] on the assumption of small elastic strain. Activation of the annular dielectric elastomer that surrounds the passive hole can reduce the hole radius by $\Delta a(V)$ following Ref. [25,26]:

$$\Delta a(V) = \frac{\nu}{1 - \nu} \frac{P_e}{E} \left[b + \frac{a^2}{b} - 2a - \nu \left(b - \frac{a^2}{b} \right) \right] \quad (3)$$

where b is the half-pitch between holes (see **Figure 2 (c-e)**).

A micro-perforated membrane acoustic absorber can be roughly represented by unit cells of Helmholtz resonators [27-29]. A Helmholtz resonator is a container of air with a neck-like open hole.

When disturbed by the sound, the air in the container or the open hole can vibrate and bounces at a fixed resonant frequency (like a spring-mass system does) to dissipate acoustic energy into heat. According to Ref. [29], this resonant frequency of air vibration is determined from the formula

$$f = \frac{c}{2\pi} \sqrt{\frac{A}{SL}}, \quad (4)$$

where c is the sound speed, A and L are the cross-sectional area and length of the neck-like open hole, and S is the volume space of the air container. Here, the hole size, i.e. $A = A(V) = \pi a^2(V)$ and $L = L(V)$ is electrically tunable by a dielectric elastomer actuator.[30,31]

3. Experiments

Fabrication of this multifunctional smart window follows the same procedures as making a dielectric electrode actuator. But, transparency tunable window device uses microwrinkled electrodes, [32] which involves the special use of TiO_2 and PEDOT:PSS nanometric thin films as the surface scatterer. Fabrication steps include (see **Figure 3(a)**): 1) biaxially pre-stretching tape of acrylate elastomer (3M VHB4905) elastomer membrane substrate three times; 2) e-beam evaporation of 19.8nm thick TiO_2 film; 3) spin coating of 38.79nm thick PEDOT:PSS film at 1000 rpm for 1 minute (Clevios P Jet HC V2, from Heraeus Deutschland GmbH & Co. KG). 3) The optical thin films were radially compressed to form microwrinkles when the elastomer membrane has the pre-stretch partially released from 3.0 times to 2.7 times. Completion of these steps and membrane transfer to rigid window frame yields a complete device, which has aluminium leads to the power supply and electronic instrumentation during testing. The device is subjected to various testing, which includes electromechanical activation using high voltage power supply (TREK 610E), and measurement for morphology, optical transmittance (using a spectrometer from AvaSpec (USB2 Fiber Optic)) (see **Figure 3(c)**) and light scattering using CMOS sensor of a digital camera, Sony 5100, which was placed at a distance of 20mm from the device.

Figure 3(b) shows the fabrication steps for making an MPDEA. First, adhesive tape of acrylate dielectric elastomer (VHB 4910) was pre-stretched radially for 3 times to have a $125.0\mu\text{m}$ membrane thickness. Later the pre-stretched membrane was transferred and adhesively bonded to a rigid ring frame of a 20.5mm internal diameter and a 28mm external diameter. The pre-stretched elastomer membrane was left 24 hours to relax and let the viscoelastic creep settle to a steady-state of deformation. Second, the aqueous conductive ink of PEDOT:PSS suspension was inkjet printed on the substrate of the pre-stretched membrane. Printing twice and subsequent drying yield a pair of transparent polymeric compliant electrodes sandwiching the dielectric elastomer membrane. **Figure 2(c)** shows a circular electrode of 20mm diameter printed on a VHB substrate, except 9 uncoated minor disk areas within it. These 9 uncoated disk areas were arranged in an orthogonal array with equal spacing of $2b=5\text{mm}$. Finally, a laser cutting machine (Epilog Helix 24) was used to laser drill through the uncoated membrane areas to produce a micro-perforated DEA (MPDEA). The average diameter of the laser-drilled holes is $2a = 447.5 \pm 30.78\mu\text{m}$. **Figure 3(d)** shows an acoustic impedance tube being used to measure the acoustic absorption spectrum of a tunable absorber at normal incidence. The 500mm long and 20mm diameter tube has a loudspeaker installed at one end and the tunable absorber mounted at the other end. Two electret array microphones (PCB piezotronic, model 130E20), which were spaced at a 20mm distance, were used to measure the sound pressure in the tube. In this setup for acoustic testing, a data logger NI PXI 6221 was used for data recording; while a high voltage amplifier (Trek model 20/20C) was used for driving a device of MPDEA.

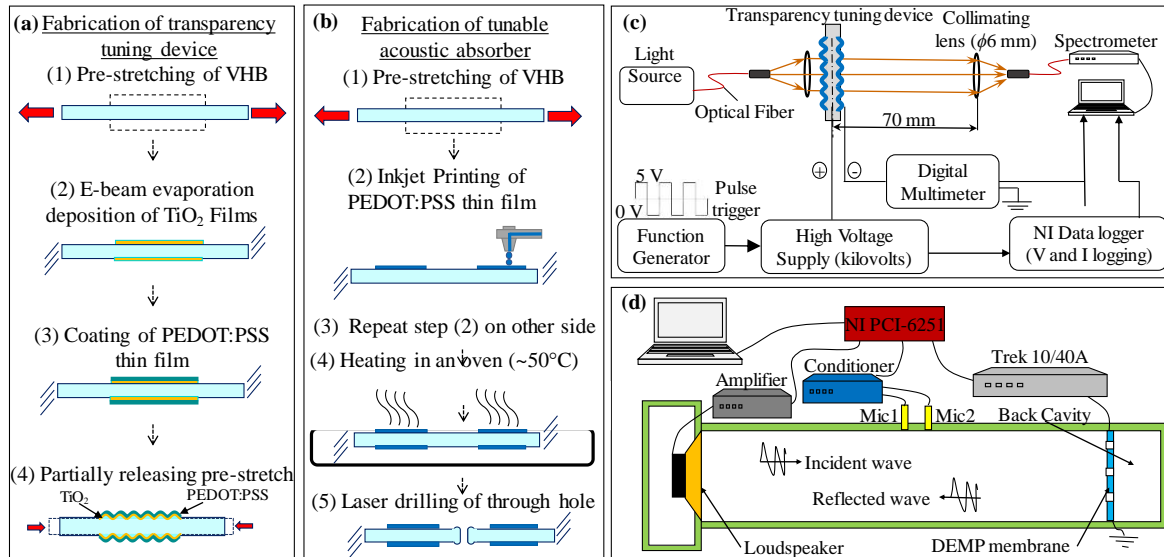


Figure 3. Fabrication procedure of the (a) Transparency tuning device; (b) tunable acoustic absorber; Measurement setup at various activation voltage for (c) optical inline transmittance measurement; (d) normal acoustic absorption.

4. Results and Discussion

The proposed device consists of two different parallel DEA membranes for two functionalities. The performance of these individual membranes is presented in the following subsections.

4.1. Transparency tuning device

The device under test is a 45 mm diameter circular dielectric elastomer actuator with 20.0 mm diameter microwrinkled electrodes. As the elastomer's radial pre-stretch is partially released from 3.0 times to 2.7 times, they buckle the hybrid multilayer thin films into microwrinkles. **Figure 4(a)** shows this microwrinkled $\text{TiO}_2/\text{PEDOT:PSS}$ electrodes in a herringbone pattern under a low pre-compression of 4-5% strain ($D_{II}/D_I=0.96$). Then, the average amplitude of the microwrinkles is $0.585\pm 0.085\mu\text{m}$ while the whole field rms roughness is $0.525\mu\text{m}$. Complete unfolding ($D(V)/D_I=1.0$) of the microwrinkled surface can reduce the rms roughness down to approximately $0.036\mu\text{m}$.

Figure 4(a-g) also shows the tunable window device can electrically vary the visibility of a logo (i.e. a laser-printed USAF resolution test chart) behind the device. When this tunable device is switched on from 0kV to 2.85kV, the diameter ratio increases from $D_{II}/D_I \sim 0.96$ towards 1.0 (see **Figure 4(g)**) and thus the microwrinkled surfaces are unfolded. The inline transmittance (for the green light of 550nm wavelength) increases from 1.85-3.0% to 78-81%. In addition, the unfolding shows a broadband effect on increasing specular (inline) transmittance (see **Figure 4(b)**). The measured specular transmittance is closely correlated to the rms surface roughness (see **Figure 4(c)**). Best fit by Equation (1) to the measurement yields the determination of an effective refractive index being $n_2 = 1.6$, higher than $n_2 = 1.47$ of VHB acrylic elastomer [33]. This enhanced light diffusion confirms a TiO_2 nanometric film being a stronger surface scatterer than the elastomer substrate. In addition, we measured the angle of light scattering by shining a collimated light beam (of a 635nm wavelength laser) through this tunable optical diffuser. **Figure 4(f)** shows a scattering angle of 44.77-degree (full width at half maximum) at the device's frosted state but almost no scattering at the device's clear state.

In terms of speed, the switch to clarity takes 60 seconds (90% rise time); whereas, the return to translucence takes 2 seconds. This suggests that a faster elastic recoil (wrinkling back) takes place at the thin-film-coated surface while a slow deactivated creep happens to the bulk viscoelastic elastomer. To demonstrate life-long cyclic switching we activated and deactivated the window device with a train of high-voltage square pulses (2.85kV amplitude, 50% duty cycle, and a pulse-on width of 1 minute) (see **Figure 4(g)**). This accelerated test for one thousand cycles confirms that the TiO_2

interfaces remain intact over repeated cycles of unfolding and wrinkling. At the activated clear state, this window device consumes merely a $0.831\text{W}/\text{m}^2$ area-specific electrical power despite high-voltage activation. Since it was first prepared four months ago, this tunable window device can still function for long-hour activation.

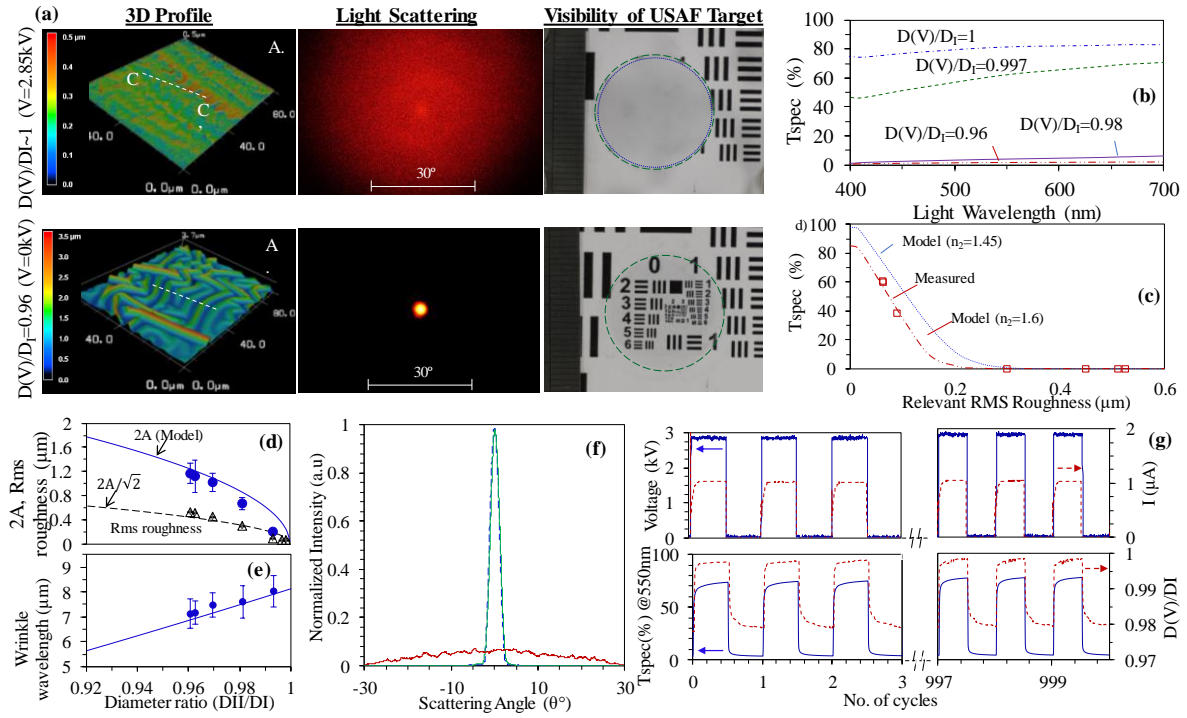


Figure 4. Theoretical and experimental results for the transparency tuning device. (a) Surface morphology and consequent light diffusion and visibility of the microwrinkled device; (b-c) In-line transmittance through the device at various diameter ratio and surface roughness; (d-e) dependence of the surface roughness and wavelength on the diameter ratio of the device; (f) light scattering angle of the device at active (green line) and inactive (red line) states; (g) In-line transmittance, diameter ratio and leakage current through the devices at oscillating ON and OFF states for 1000 cycles.

4.2 Tunable acoustic absorber

Figure 5(a & d) shows that MPDEAs with inkjet-printed PEDOT:PSS electrodes are slightly bluish yet optically clear with close to 78.64% optical transmittance throughout the visible spectrum. The electrical activation of MPDEAs reducing the perforation hole from an inactivated diameter $2a_0 = 447.5 \pm 30.78\mu\text{m}$ to a smaller activated diameter $2a(V)$. The MPDEA can be driven up to 4kV to reduce the hole diameter by 10%. It consumes $1.27\text{watt}/\text{m}^2$ electrical power at the activated state. **Figure 5(e)** shows the absorption spectrum of MPDEA-based tunable acoustic absorbers. In the inactivated state, the bandwidth for the above 0.8 acoustic absorption coefficient is 349 Hz (from 831 Hz to 1180 Hz). The peak absorption happens at 1055 Hz upon inactivation (0kV) but shifted by 18.5% to 860 Hz upon 5.0kV activation.

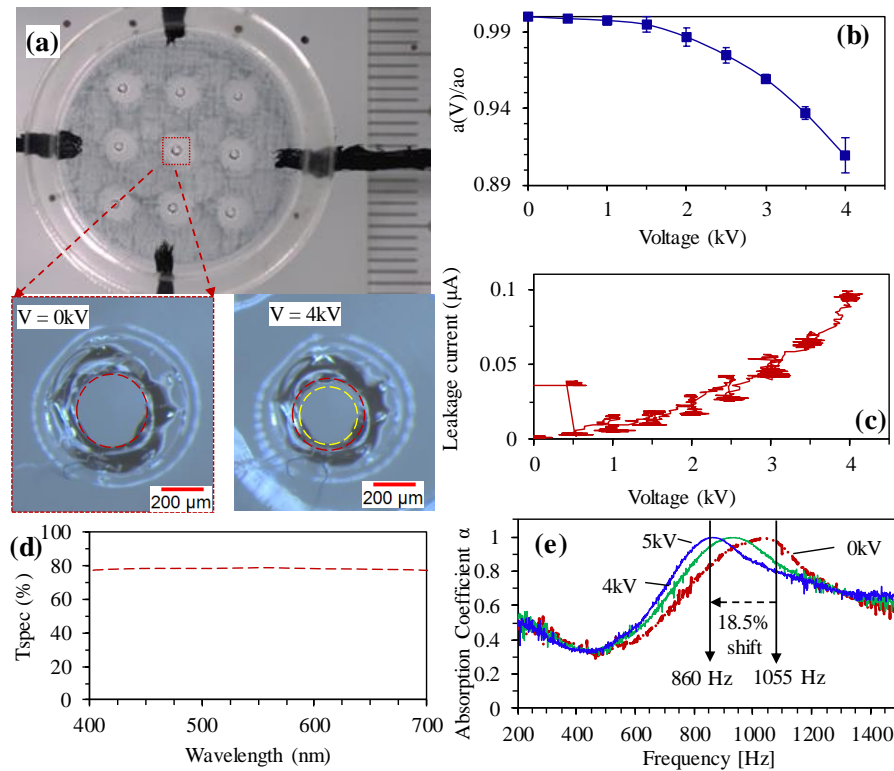


Figure 5. Theoretical and experimental results for the tunable window device. (a) Front view of the device with magnified views of the holes at active and inactive states; (b-c) dependence of the hole diameter and leakage current on the applied voltage; (d) optical transmittance of the device; (e) acoustic spectrum of the device at various activation voltage.

5. Conclusions

This work presented a multi-layered solution for tunable optical and acoustic window based on dielectric elastomer actuators and transparent wrinkleable compliant electrodes. The first layer is for transparency tuning and its surface roughness is varied employing surface micro-wrinkling or unfolding. As small strain-induced microwrinkling and unfolding is wished to make smart glasses, this work showed microwrinkling of nanometric films of TiO_2 of high refractive index are effective to diffuse light down to 1-2% inline transmittance (very frosted) upon less than 5% axial compressive strain. Interestingly, these brittle oxide thin films can sustain thousands of cyclic microwrinkling and unfolding. A conductive overcoat on the oxide film made of the conductive polymer provides electrical conductivity. Such multilayer thin film can make microwrinkled compliant electrode suitable for activating DEA and thus generates voltage induced unfolding. Moreover, this device also showed prominent improvements in terms of power consumption (consumes merely $\sim 0.831\text{ W/m}^2$).

The sound-absorbing layer based on micro-perforated dielectric elastomer actuator can absorb mid-frequency sound while being optically clear (up to 78.64% light transmission). The need for tuning the resonant frequency to match the noise dominant frequency can only be addressed using an MPDEA. We devised a mechanism of tuning hole-diameter by activation of an MPDEA. Unlike other actuators such as an electric motor or mechanical switches, MPDEA provides a distributed and quiet actuation. Such novel smart windows can be made as cheap as glass due to its simple all-solid-state construction. They can be arranged in an array for large area mounting to the window glass. Advances of such transparent tunable acoustic absorbers are anticipated to bring good quality acoustics and natural lighting to the indoor space.

Acknowledgements: This research was supported by Singapore Millennium Foundation managed by Temasek Foundation Innovates and by Temasek Foundation Ecosperity.

Author Contributions: M.S., Z.L., A.A. and G.-K.L. conceived the idea and designed the study. M.S. contributed to all the material design and device fabrication. M.S. and Z.L. designed the experimental setup and conducted

the acoustic testing. M.S., Z.L., and G.-K.L. carried out the data analysis. M.S., Z.L. and G.-K.L. derived the models. M.S. wrote the manuscript. All the authors discussed the results and revised the manuscript.

Conflicts of Interest: The authors declare no competing financial interest.

Abbreviations

The following abbreviations are used in this manuscript:

DEA: Dielectric elastomer actuators

MPP: Microperforated panel

MPDEA: Microperforated dielectric elastomer actuator

References

1. Cox, T.J.; D'antonio, P. *Acoustic absorbers and diffusers: theory, design and application*; Crc Press: 2009.
2. Gerriets-GmbH. Absorber Light. Available online: <https://www.gerriets.com/us/absorber-light-8172> (accessed on
3. Lampert, C.M. Chromogenic smart materials. *Materials today* **2004**, *7*, 28-35.
4. Granqvist, C.G. Electrochromics for smart windows: Oxide-based thin films and devices. *Thin Solid Films* **2014**, *564*, 1-38.
5. Doane, J.W.; Vaz, N.A.; Wu, B.G.; Žumer, S. Field controlled light scattering from nematic microdroplets. *Applied Physics Letters* **1986**, *48*, 269-271, doi:10.1063/1.96577.
6. Drzaic, P.S. Polymer dispersed nematic liquid crystal for large area displays and light valves. *Journal of applied physics* **1986**, *60*, 2142-2148.
7. Baetens, R.; Jelle, B.P.; Gustavsen, A. Properties, requirements and possibilities of smart windows for dynamic daylight and solar energy control in buildings: A state-of-the-art review. *Solar Energy Materials and Solar Cells* **2010**, *94*, 87-105.
8. van den Ende, D.; Kamminga, J.D.; Boersma, A.; Andritsch, T.; Steeneken, P.G. Voltage-controlled surface wrinkling of elastomeric coatings. *Advanced materials* **2013**, *25*, 3438-3442, doi:10.1002/adma.201300459.
9. Görrn, P.; Cao, W.; Wagner, S. Isotropically stretchable gold conductors on elastomeric substrates. *Soft Matter* **2011**, *7*, 7177, doi:10.1039/c1sm05705g.
10. Zang, J.; Ryu, S.; Pugno, N.; Wang, Q.; Tu, Q.; Buehler, M.J.; Zhao, X. Multifunctionality and control of the crumpling and unfolding of large-area graphene. *Nature materials* **2013**, *12*, 321-325, doi:10.1038/nmat3542.
11. Ong, H.-Y.; Shrestha, M.; Lau, G.-K. Microscopically crumpled indium-tin-oxide thin films as compliant electrodes with tunable transmittance. *Applied Physics Letters* **2015**, *107*, 132902, doi:10.1063/1.4932115.
12. Thomas, A.V.; Andow, B.C.; Suresh, S.; Eksik, O.; Yin, J.; Dyson, A.H.; Koratkar, N. Controlled crumpling of graphene oxide films for tunable optical transmittance. *Advanced materials* **2015**, *27*, 3256-3265, doi:10.1002/adma.201405821.
13. Kang, J. An acoustic window system with optimum ventilation and daylighting performance. *Noise & Vibration Worldwide* **2006**, *37*, 9-17.
14. Asdrubali, F.; Pispola, G. Properties of transparent sound-absorbing panels for use in noise barriers. *The Journal of the Acoustical Society of America* **2007**, *121*, 214-221, doi:10.1121/1.2395916.
15. Struiksmā, A.; Tenpierik, M.; Snijder, A.; Veer, F.; Botterman, B.; Hornikx, M.; van der Water, H.; Migchielsen, F. Sound absorbing glass: transparent solution for poor acoustics of monumental spaces. *SPOOL* **2017**, *4*, 53-58.

16. Soundproofing-windows.net. Soundproofing Windows with Double and Triple Glazing. Available online: <http://soundproofing-windows.net/index.php/soundproofing-windows-with-double-and-triple-glazing> (accessed on
17. Shrestha, M.; Lau, G.-K. Tunable window device based on micro-wrinkling of nanometric zinc-oxide thin film on elastomer. *Optics letters* **2016**, *41*, 4433, doi:10.1364/ol.41.004433.
18. Shrestha, M.; Asundi, A.; Lau, G.-K. Smart Window Based on Electric Unfolding of Microwrinkled TiO₂ Nanometric Films. *ACS Photonics* **2018**, 10.1021/acsp Photonics.8b00486, doi:10.1021/acsp Photonics.8b00486.
19. Beckmann, P.; Spizzichino, A. The scattering of electromagnetic waves from rough surfaces. *Norwood, MA, Artech House, Inc., 1987*, 511 p. **1987**.
20. Eastman, J. Surface scattering in optical interference coatings. **1974**.
21. Zeman, M.; van Swaaij, R.A.C.M.M.; Metselaar, J.W.; Schropp, R.E.I. Optical modeling of a-Si:H solar cells with rough interfaces: Effect of back contact and interface roughness. *Journal of Applied Physics* **2000**, *88*, 6436-6443, doi:10.1063/1.1324690.
22. Keplinger, C.; Sun, J.-Y.; Foo, C.C.; Rothenmund, P.; Whitesides, G.M.; Suo, Z. Stretchable, transparent, ionic conductors. *Science* **2013**, *341*, 984-987.
23. Lang, U.; Naujoks, N.; Dual, J. Mechanical characterization of PEDOT:PSS thin films. *Synthetic Metals* **2009**, *159*, 473-479, doi:10.1016/j.synthmet.2008.11.005.
24. Lau, G.-K.; Heng, K.-R.; Ahmed, A.S.; Shrestha, M. Dielectric elastomer fingers for versatile grasping and nimble pinching. *Applied Physics Letters* **2017**, *110*, 182906, doi:10.1063/1.4983036.
25. Lu, Z.; Shrestha, M.; Lau, G.-K. Electrically tunable and broader-band sound absorption by using micro-perforated dielectric elastomer actuator. *Applied Physics Letters* **2017**, *110*, 182901, doi:10.1063/1.4982634.
26. Shrestha, M.; Lu, Z.; Lau, G.-K. Transparent tunable acoustic absorber membrane using inkjet printed PEDOT: PSS thin-film compliant electrodes. *ACS applied materials & interfaces* **2018**, 10.1021/acsa mi.8b12368, doi:10.1021/acsa mi.8b12368.
27. Maa, D.-Y. Potential of microperforated panel absorber. *Journal of the Acoustical Society of America* **1998**, *104*.
28. D. Herrin; J. Liu. Properties and applications of microperforated panels. *Sound and Vibrations* **2011**.
29. Ginn, K. *Architectural acoustics*; Brüel & Kjaer: 1978.
30. Shian, S.; Clarke, D.R. Electrically tunable window device. *Optics letters* **2016**, *41*, 1289-1292, doi:10.1364/OL.41.001289.
31. Rosset, S.; Shea, H.R. Flexible and stretchable electrodes for dielectric elastomer actuators. *Applied Physics A* **2012**, *110*, 281-307, doi:10.1007/s00339-012-7402-8.
32. Low, S.H.; Lau, G.K. Bi-axially crumpled silver thin-film electrodes for dielectric elastomer actuators. *Smart Materials and Structures* **2014**, *23*, 125021.
33. 3M. *Converting 3M Technology into Successful Applications*. 2015.



© 2020 by the authors; licensee MDPI, Basel, Switzerland. This article is an open access article distributed under the terms and conditions of the Creative Commons by Attribution (CC-BY) license (<http://creativecommons.org/licenses/by/4.0/>).